JOURNAL OF AGRICULTURAL AND FOOD CHEMISTRY

Article

pubs.acs.org/JAFC

Allicin Induces Anti-human Liver Cancer Cells through the p53 Gene Modulating Apoptosis and Autophagy

Yung-Lin Chu,[†] Chi-Tang Ho,[†,‡] Jing-Gung Chung,[§] Rajasekaran Raghu,[∥] Yi-Chen Lo,[†] and Lee-Yan Sheen*[,†,⊥,#]

[†]Institute of Food Science and Technology, [∥]Department of Horticulture and Landscape Architecture, [⊥]National Center for Food Safety Education and Research, and [#]Center for Food and Biomolecules, National Taiwan University, Number 1, Section 4, Roosevelt Road, Taipei 106, Taiwan

[‡]Department of Food Science, Rutgers, The State University of New Jersey, 65 Dudley Road, New Brunswick, New Jersey 08901, United States

[§]Department of Biological Science and Technology, China Medical University, Number 91, Hsueh-Shih Road, Taichung 404, Taiwan

Supporting Information

ABSTRACT: Hepatocellular carcinoma (HCC) is the most prevalent type of liver cancer globally and ranks first among the cancer-related mortalities in Taiwan. This study aims to understand the modes of cell death mechanism induced by allicin, a major phytochemical of crushed garlic, in human hepatoma cells. Our earlier study indicated that allicin induced autophagic cell death in human HCC Hep G2 ($p53^{wild\ type}$) cells, whereas in the present study, allicin induced apoptotic cell death through caspase-dependent and caspase-independent pathways by reactive oxygen species (ROS) overproduction in human HCC Hep 3B ($p53^{mutation}$) cells. To gain insight into the cell death mechanism in p53 knocked down Hep G2, we silenced the p53 gene using siRNA-mediated silencing. Allicin treatment induced apoptotic cell death in p53 knocked down Hep G2 cells similar to that of Hep 3B cells. These results suggest that allicin induced cell death in human hepatoma cells through either autophagy or apoptosis and might be a potential novel complementary gene therapeutic agent for the treatment of apoptosis-resistant cancer cells.

KEYWORDS: *Allicin, apoptosis, autophagy, p53, reactive oxygen species*

INTRODUCTION

Phytochemicals present in the human diet have attracted much attention for their health-related potential and chemoprevention of cancer. Garlic (*Allium sativum*), the legendary vegetable or spice, is bestowed with numerous health beneficial functions, such as antibiotic,[1] antivirus,[2] antiplatelet aggregation,[3] antiatherosclerotic,[4] antiproliferative,[5] and anti-fatty liver properties.[6] The predominant component of garlic, allicin is biosynthesized from its precursor alliin by alliinase. Allicin has been extensively studied for its wide range of biological activity, including anticancer.[7]

Viral hepatitis can induce acute and chronic inflammation of the liver, leading to cirrhosis, and is the major risk factor leading to liver cancer. Nearly 70% of liver carcinoma cases are induced by hepatitis B and C, and liver cancer is the leading cancer death in Taiwan. In the present research, we focus on the effect of allicin treatment on human hepatoma Hep 3B cells, which contain an integrated hepatitis B virus genome and p53 gene mutation.

Cell deaths include program cell death-I (PCD-I), also called apoptosis, program cell death-II (PCD-II), also called autophagy,[8] and non-program cell death, normally referred to as necrotic cell death. To validate p53-gene-mediated regulation of PCD in human liver cancer cells, this study focuses on the effect of allicin treatment on p53-mutation (Hep 3B cells) and p53-wild type (Hep G2 cells) human liver cancer cells.

Reactive oxygen species (ROS) featured by uncoupling electrons, including H_2O_2, $O_2^{\bullet -}$, $^1O_2$, and $^{\bullet}OH$, formed by endogenous sources and environmental factors. Normally, ROS maintains homeostasis in our body. Imbalance of cellular ROS leads to the injury of cellular structures. However, some studies suggest that tumor cells have their own threshold of ROS levels higher than that of normal cells. Upon drug treatment to tumor cells, it may induce ROS production to exceed the survival threshold of tumor cells and trigger tumor death.[9]

It has been well-established that cancer cells have acquired an innate ability to escape apoptosis, and the number of genetic mutations have damaged their genes, such as p53. There are over 50% cancer cells with p53 gene mutation, deletion, or non-function. However, p53 gene is an important tumor suppressor gene, which involves in many physiological functions, such as cell death, stress, cell cycle, cell differentiation, and immune response. Therefore, it will exert a great influence in suicide gene therapy for cancer cells with or without p53 gene function.[10] It has been reported that garlic could regulate some suicide genes in cancer treatment.[11] However, there is no study demonstrating how allicin mediates various cell death models by p53 gene. The objectives of this study are to elucidate the

Received: July 23, 2013
Revised: September 23, 2013
Accepted: September 23, 2013
Published: September 23, 2013

role of allicin in the regulation of different types of cell death in human liver cancer cells and to determine the potential of garlic in complementary suicide gene therapy in human liver cancer.

MATERIALS AND METHODS

Chemicals and Reagents. Allicin, dimethyl sulfoxide (DMSO), propidium iodide (PI), RNase A, Tris-HCl, potassium phosphates, *N*-acetylcysteine (NAC), 3-methyladenine (3-MA), Triton X-100, and trypan blue were purchased from Sigma-Aldrich Chemical (St. Louis, MO). The fluorescent probe 2,7-dichlorodihydrofluorescein diacetate (DCFH-DA), Mito Tracker-Red, 4′,6-diamidino-2-phenylindole (DAPI), glycine, *N*-[4-[6-[(acetyloxy)methoxy]-2,7-dichloro-3-oxo-3*H*-xanthen-9-yl]-2-[2-[2-[bis[2-[(acetyloxy)methoxy]-2-oxyethyl]-amino]-5-methylphenoxy]ethoxy]phenyl]-*N*-[2-[(acetyloxy)-methoxy]-2-oxyethyl]-, (acetyloxy)methyl ester/121714-22-5 (Fluo-3/AM), and 3,3′-dihexyloxacarbocyanine iodide ($DiOC_6$) were purchased from Invitrogen Life Technologies (Carlsbad, CA). Dulbecco's modified Eagle's medium (DMEM) with 2 mM L-glutamine, fetal bovine serum (FBS), penicillin−streptomycin, and trypsin−ethylenediaminetetraacetic acid (EDTA) were obtained from Gibco BRL (Grand Island, NY). Materials and chemicals for gel electrophoresis were from BioRad (Hercules, CA). Annexin V-FITC/PI Apoptosis Detection Kit I was procured from BD Biosciences (San Jose, CA), and Polysine microscope adhesion slides were obtained from Thermo Fisher Scientific, Inc. (Waltham, MA).

The qualitative and quantitative analyses of allicin were performed as described in our previous study.[12]

Cell Culture. Human liver carcinoma Hep 3B ($p53^{mutation}$) and Hep G2 ($p53^{wild\ type}$) cell lines were obtained from the Department of Medical Research and Education, Taipei Veterans General Hospital, Taipei, Taiwan. Hep 3B cells were placed into a 10 cm^2 dish with DMEM supplemented with 10% FBS, 2 mM L-glutamine, 100 units/mL penicillin, and 100 μg/mL streptomycin and grow under humidified 5% CO_2 and 95% air at 37 °C. Adherent cells were suspended by 1 mL of 1% trypsin−EDTA for 5 min at 37 °C.

Determination of Cell Morphology, Viability, Cell Cycle, and sub-G1 Phase. Hep 3B cells were seeded at a density of 1×10^5 cells/well in a 12-well plate. The seeded cells were incubated with 0, 15, 20, 25, 35, 40, and 50 μM allicin for 24 h at 37 °C and 5% CO_2 and 95% air. The morphological changes were directly examined and photographed by a phase-contrast microscope at 200× magnification. The percentage of viable cells was determined by flow cytometry (Becton-Dickinson, San Jose, CA) after centrifugation of the cells and resuspension in phosphate-buffered saline (PBS) containing PI (5 μg/mL). For cell cycle distribution and sub-G1 determination, isolated cells were fixed gently by 70% ethanol overnight at 4 °C, resuspended in PBS containing 50 μg/mL PI, 0.1 mg/mL RNase A, and 0.1% Triton X-100 in a dark room for 30 min at 37 °C, and then analyzed with a flow cytometer with Modfit LT, version 2.0 (Verity Software House, Topsham, ME). Cells treated with 0.1% DMSO served as the control.

DAPI Staining. For DAPI staining, approximately 5×10^4 cells/mL of Hep 3B cells in a 6-well plate were treated with 0, 20, 25, 35, 40, and 50 μM allicin for 24 h. Cells were stained with DAPI, then examined, and photographed using a fluorescence microscope as described elsewhere.[13] The nuclei was labeled by DAPI staining, in which it was visualized by excitation at 330−385 nm and emission at 420 nm.

Detections of ROS and Mitochondrial Membrane Potential (ΔΨm) in Hep 3B Cells. Approximately 1×10^5 cells/mL of Hep 3B cells were treated with 35 μM allicin for 1, 3, and 6 h, and the cells were resuspended in 500 μL of PBS with 10 μM DCFH-DA for ROS and in 500 μL PBS with 4 μmol/L $DiOC_6$ for ΔΨm. Cells were incubated at 37 °C in the dark for 30 min before flow cytometry analysis.

Apoptosis Assay. To examine if allicin treatment induced apoptosis in Hep 3B cells, we seeded cells at a concentration of 1×10^5 cells/well in a 12-well plate and performed an annexin V-FITC/PI double-staining apoptosis assay. The cells were treated with 35 μM allicin for 0, 6, 12, and 24 h and then washed twice with PBS buffer. Then, we resuspended Hep 3B cells in 1× binding buffer with 1×10^6 cells/mL and transferred 100 μL of 1× binding buffer with 1×10^5 cells/mL to a 5 mL fluorescence-activated cell sorting (FACS) tube. The following steps were performed in the dark. To the FACS tubes, 5 μL of annexin V-FITC and 10 μL of PI were added. Finally, after the addition of 400 μL of 1× binding buffer, samples were analyzed by flow cytometry within 1 h.

Analysis of Protein Expression by Western Blotting. Hep 3B cells plated at a density of 1×10^7 cells on a 10 cm^2 dish were treated with 35 μM allicin for 0, 3, 6, 12, 24, and 48 h for examining key proteins correlated with apoptosis, DNA damage, and endoplasmic reticulum (ER) stress signaling. For western blot analysis, total proteins (25 μg) of cell lysates were separated on a 12% sodium dodecyl sulfate−polyacrylamide gel electrophoresis (SDS−PAGE) for 90 min and transferred to nitrocellulose membrane (Millipore, Billerica, CA). The blot was soaked in blocking buffer [5% non-fat dry milk/0.05% Tween-20 in 20 mM Tris-buffered saline (TBS) at pH 7.6] at room temperature for 1−1.5 h and incubated with individual primary monoclonal antibodies: HtrA2, B-cell lymphoma 2 (Bcl-2), Bcl-2-associated X protein (Bax), caspase 9, apoptotic-induced factor (AIF), endonuclease G (Endo G), caspase 3, PARP, γ-H_2AX, and caspase 8 (Cell Signaling Technology, Danvers, MA), in nonfat milk blocking buffer at 4 °C for over 4 h. After washing twice with TBS, the blots were treated with horseradish-peroxidase-conjugated secondary antibody for detection by WesternBreeze chemiluminescent kit (Invitrogen) according to the instructions of the manufacturer. Anti-β-actin (a rabbit monoclonal antibody) served as an internal control.

Translocation for AIF and Endo G Protein into the Nucleus Detected by Confocal Laser Scanning Microscopy. Hep 3B cells at a density of 5×10^4 cells/well cultured on Polysine microscope adhesion slides (Cel-line, Thermo) were treated with or without 35 μM allicin for 24 h, fixed in 4% paraformaldehyde in PBS for 15 min, and permeabilized with 0.1% Triton-X 100 in PBS for 0.5 h with blocking of non-specific binding sites using 2% bovine serum albumin (BSA) as described.[14] The fixed cells were stained overnight with primary antibodies of AIF and Endo G (1:100 dilution) (green fluorescence). Subsequently, they were washed twice with PBS and stained with secondary antibody (FITC-conjugated goat anti-mouse IgG at 1:100 dilution), followed by staining with PI (red fluorescence) for DNA as described previously. All samples were visualized and photographed using a Leica TCS SP5 II confocal spectral microscope.

γ-H_2AX Foci Formation Measured by an Immunostaining Method. Hep 3B cells were placed on Polysine microscope adhesion slides (Cel-line, Thermo) and treated with 35 μM allicin. At different time points (0, 3, 6, 12, and 24 h), cells were fixed in 4% paraformaldehyde/PBS and stained with anti-phospho γ-H_2AX (ser139 clone, Cell Signaling) according to the dilution of the data sheet. A γ-H_2AX foci image was acquired on a Leica TCS SP5 II confocal laser scanning microscope. All image data were quantified by Image J software, an image-inspired Java program from the National Institute of Health (NIH).

Acridine Orange (AO) Staining for Autophagy Assays. AO is the common method of detecting autophagy. It is used to measure proton-pump-driven lysosomal acidity and generates a significant pH gradient, resulting in the efficient concentration of AO within the lysosome organelles. The effectiveness of this AO concentration process is sufficient to create intralysosomal concentrations, leading to precipitation of the AO into aggregated granules. Allicin-treated Hep 3B cells were stained with AO (1 μg/mL, Sigma) for 15 min at 37 °C, with analysis by flow cytometry.

Confocal Laser Scanning Microscopy for the Autophagosome of LC3-II-FITC Punctate Formation. Hep 3B liver cancer cells at a density of 5×10^4 cells/well were seeded on Polysine microscope adhesion slides (Cel-line, Thermo) and then were treated with or without 35 μM allicin. Then, cells on the slides were fixed at various time points in 4% paraformaldehyde in PBS for 15 min and permeabilized with 0.1% Triton-X 100 in PBS for 0.5 h with blocking of non-specific binding sites using 5% blocking buffer. The fixed cells were stained overnight at 4 °C with primary antibodies to LC3-II

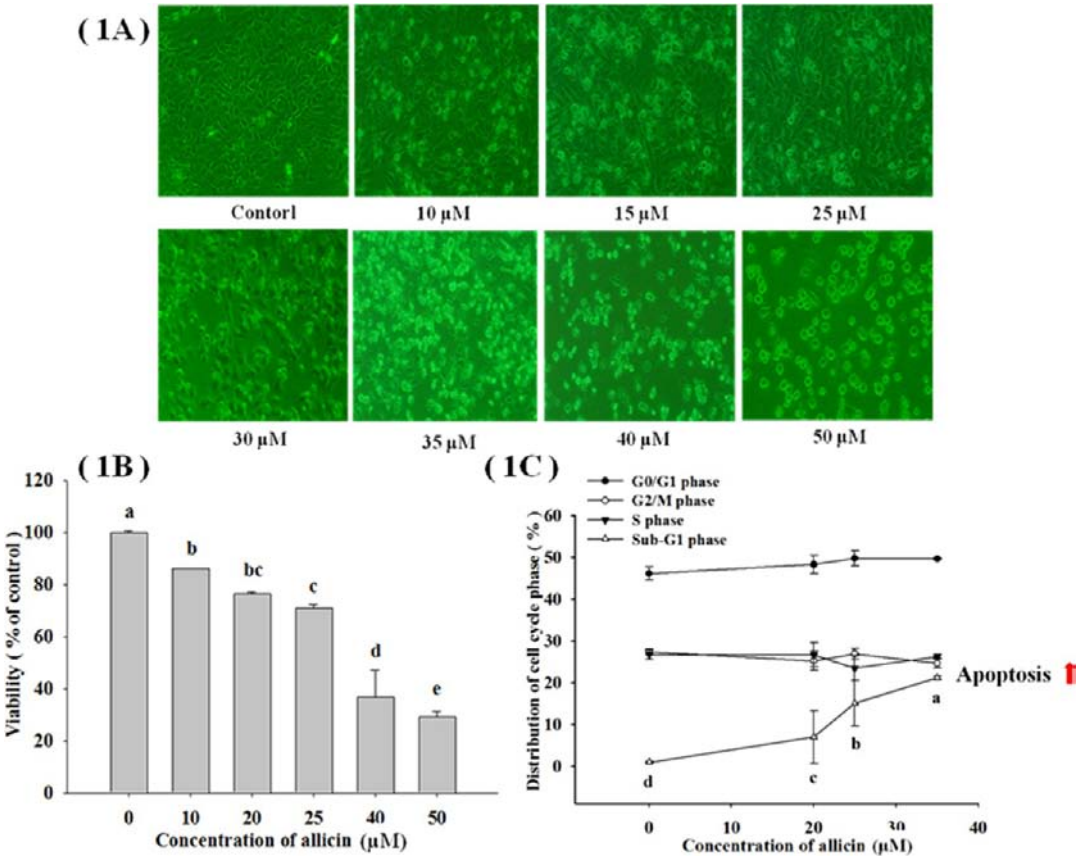

Figure 1. (A) Effect of the allicin concentration on the morphology of Hep 3B cells after 24 h under a light microscope (400×). (B) Viability of Hep 3B cells after 24 h of allicin by flow cytometric analysis. The IC_{50} of allicin treated with Hep 3B cells is about 35 μM. Data are expressed as the mean ± SD (n = 3) and analyzed statistically using one-way ANOVA and Duncan's test. Different letters (a–e) represent statistically significant differences among treatments (p < 0.05). (C) Cell cycle distribution in Hep3B cells on allicin treatment. The cells were labeled with PI. Hep 3B cells treated with different allicin concentrations were analyzed by flow cytometry after 24 h of incubation. Data are expressed as the mean ± SD (n = 3) and analyzed statistically using one-way ANOVA and Duncan's test. Different letters (a–d) represent statistically significant differences among treatments (p < 0.05).

(Genetex, Irvine, CA) (1:3000 dilution) (green fluorescence). Subsequently, the slides were washed twice with PBS and stained with secondary antibody (FITC-conjugated goat anti-rabbit IgG at 1:100 dilution), followed by nuclear staining with DAPI (blue fluorescence) as described previously. All samples were visualized using a Leica TCS SP5 II confocal spectral microscope. All image data were quantified by an image-inspired Java program, Image J software from the NIH.

Quantitative Real-Time Polymerase Chain Reaction (qRT-PCR). To validate the western results, qRT-PCR was performed. First-strand cDNA was synthesized as a 20 μL reaction, with 1 μg of total RNA as the template using QuantiTect reverse transcription kit (Qiagen, Hilden, Germany) according to the protocol of the manufacturers. The qPCR primers for caspase 3 (F, TCGCTTCCATGTATGATCTTTG; R, CTGCCTCTTCCCCCATTCT), AIF (F, TCTAGAGGAACATGCCATCG; R, GCTTTGAAGCAGAAGCTGGT), and β-actin (F, TGGCA CCACA CCTTC TACAA; R, GCAGC TCGTA GCTCT TCTCC) were chosen from the qPrimerDepot primer database.[15,16] β-actin was used as an endogenous control. Real-time PCR was performed on an ABI StepOne Plus Real-Time PCR System (Applied Biosystems, Foster City, CA) using KAPA SYBR FAST qPCR Kit Master Mix ABI Prism (KK4603, Kapa Biosystems, Woburn, MA). The qPCR reactions were performed with 1 μL of 5 times diluted first-strand cDNA, 1× qPCR master mix, and 200 nM of each forward and reverse primer. The PCR conditions were 95 °C for 1 min, followed by 40 cycles of 95 °C for 3 s and 60 °C for 30 s, and for verification of target gene amplifications, a dissociation stage at 95 °C for 15 s, 60 °C for 1 min, and 95 °C for 15 s. Gene expression was normalized to the endogenous control β-actin. Normalized gene expression of the allicin group was expressed relative to the control group. The expression levels were determined on four biological replicates, and each biological sample was replicated to obtain three technical replicates, employing the $2^{-\Delta\Delta C_T}$ method for gene expression.[15]

Transfection of siRNA-Tumor Protein 53 (siRNA-TP53). For the transfection experiment, Hep G2 cells were seeded in 40 mm culture dishes and grown until 80% confluence. Dharmacon ON-TARGETplus SMART pool siRNAs against human TP53 at a final concentration of 25 nM were transfected to 1.5–2.5 × 10^5 Hep G2 cells using DharmaFECT-4 transfection reagent according to the instructions of the manufacturers. At 6 h post-transfection, the transfection reagent was replaced with complete medium. Allicin (35 μM) was added to the transfected cells and incubated for 24 h at 37 °C in a 5% CO_2 incubator, after which the cells were subjected to an annexin V-FITC/PI assay. For western blotting, the transfection was carried out in 10 cm^2 plates.

Statistical Analysis. All results are reported as the mean ± standard deviation (SD), and the difference between the allicin-treated and control groups were analyzed by one-way analysis of variance (ANOVA) and Duncan's multiple comparison tests (SAS Institute, Inc., Cary, NC) to determine significant differences among treatments (p < 0.05).

RESULTS AND DISCUSSION

Garlic consumption may decrease the risk of cancer initiation and inhibit cell proliferation of gastric, colon, skin, and breast

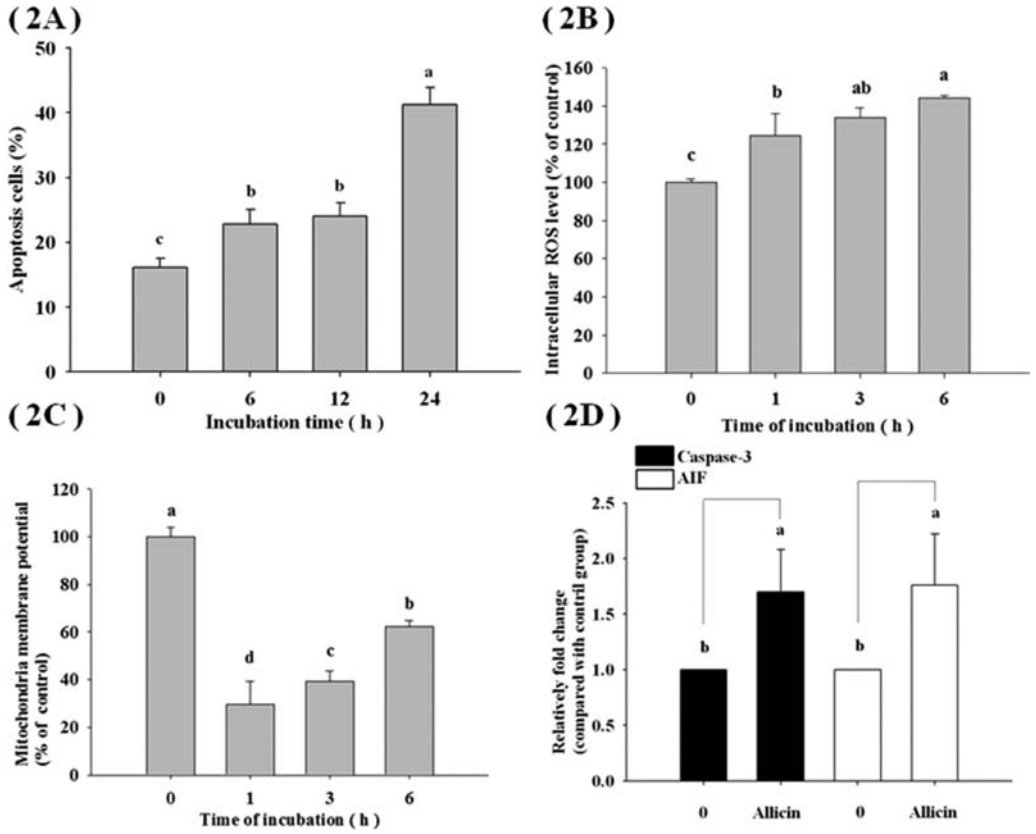

Figure 2. (A) Induction of apoptosis at various time intervals in Hep 3B cells by annexin V-FITC/PI double staining. Data are expressed as the mean ± SD (n = 3) and analyzed statistically using one-way ANOVA and Duncan's test. Different letters (a−c) represent statistically significant differences among treatments (p < 0.05). (B) Allicin increased intracellular ROS production of Hep 3B cells. The cells were labeled with DCF-DA. Hep 3B cells treated with 35 μM allicin after 1, 3, and 6 h were subjected to flow cytometric analysis. Data are expressed as the mean ± SD (n = 3) and analyzed statistically using one-way ANOVA and Duncan's test. Different letters (a−c) represent statistically significant differences among treatments (p < 0.05). (C) Allicin decreased mitochondria membrane potential of Hep 3B cells. The cells were labeled with 3,3′-dihexyloxacarbocyanine iodide ($DiOC_6$). Hep 3B cells treated with 35 μM allicin after 1, 3, and 6 h were subjected to flow cytometric analysis. Data are expressed as the mean ± SD (n = 3) and analyzed statistically using one-way ANOVA and Duncan's test. Different letters (a−d) represent statistically significant differences among treatments (p < 0.05). (D) mRNA expression of caspase 3 and AIF in Hep 3B cells after 35 μM allicin treatment at 24 h. Data are expressed as the mean ± SD (n = 3) and analyzed statistically using one-way ANOVA and Duncan's test. Different letters (a−c) represent statistically significant differences among treatments (p < 0.05).

cancer cell lines.[17−20] It is well-known that the cell death is regulated by apoptosis, necrosis, and autophagy.[21] Thus far, some studies showed that garlic or its active components, such as diallyl sulfides, induce apoptosis in cancer cell lines.[22,23] To the best of our knowledge, no studies demonstrated that garlic could regulate apoptosis, autophagy, and necrosis in hepatocarcinoma cells. We are the first to report on the validation of allicin regulating different death models in liver cancer cells.

Effect of Allicin on the Viability and Morphology of Hep 3B Cells. Allicin-induced morphological changes in Hep 3B cells as observed under a phase-contrast microscope revealed cell shrinkage (Figure 1A). The viability of Hep 3B cells was assessed by flow cytometry. The IC_{50} of allicin was determined to be 35 μM in Hep 3B cells at 24 h, and the number of viable cells changed (Figure 1B) in a dose-dependent manner after 24 h of incubation. In another study, allicin treatment did not increase the leakage of lactate dehydrogenase (LDH) of primary rat hepatocytes until 1 mM allicin treated with rat hepatocytes.[24] For this reason, allicin could be inferred as safe to normal liver cells.

Allicin Treatment Increased Distribution of Apoptotic Cells in Hep 3B Cells. Cell cycle is a key process in regulation of cells. Toward this, we used flow cytometry to study the regulation of the cell cycle distribution in Hep 3B cells after allicin treatment. From Figure 1C and Figure S1 of the Supporting Information, it is quite evident that the percentage of sub-G1 phase distribution in the whole cell cycle had increased, indicating allicin-induced genome destruction in Hep 3B cells significantly (p < 0.05).

Furthermore, Hep 3B cells labeled with annexin-V-FITC/PI exhibited an increase in the expression level of annexin-V-FITC positive cells by allicin treatment at 24 h (Figure 2A and Figure S2 of the Supporting Information). Both results indicated that allicin clearly induced apoptosis in Hep 3B cells. However, no significant apoptosis was observed in Hep G2 cells after only the allicin-treating group (panels A and B of Figure 7), and this intrigued us to explore the difference between Hep 3B and Hep G2 cells. Obviously, because the presence or absence of p53 gene is the major difference between these two hepatoma cell lines, we used siRNA-TP53 to understand the relation of the p53 gene on the regulation of apoptosis and autophagy of allicin treatment in human hepatoma cells.

Allicin Decreased Mitochondrial Membrane Potential (MMP) and Mitochondrial-Dysfunction-Related Proteins. The imbalance in ROS expression will cause damage

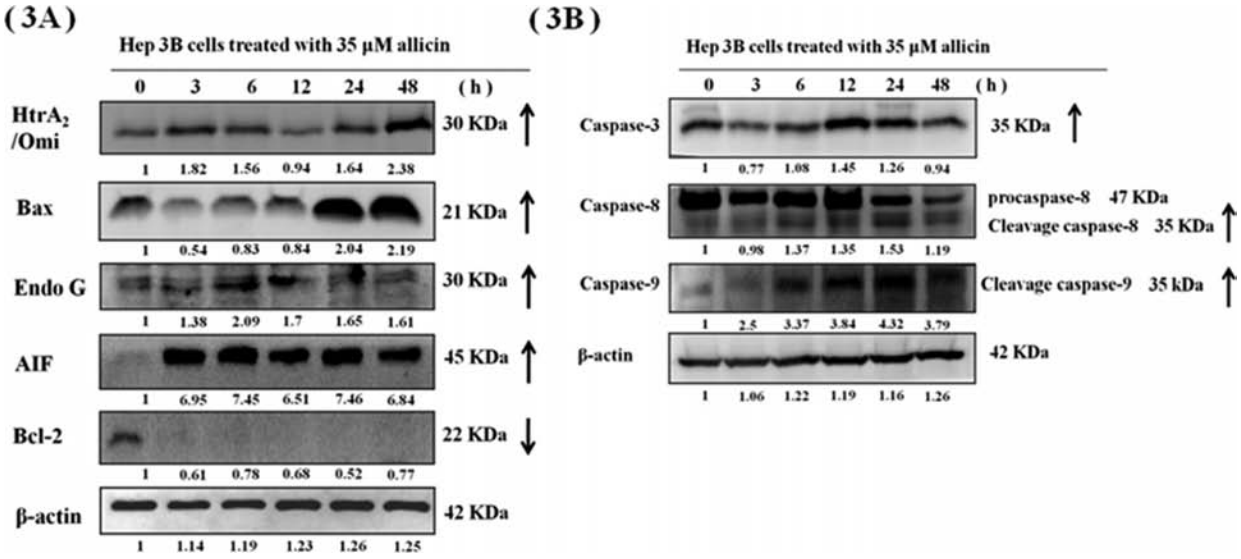

Figure 3. (A) Caspase-independent apoptosis pathway protein expression in Hep 3B cells after 35 μM allicin treatment at different time intervals. (B) Caspase-dependent apoptosis-related protein expression in Hep 3B cells after 35 μM allicin treatment at different time intervals. All proteins were quantified by densitometry on the immunoblots by Image J software, as described in the Materials and Methods.

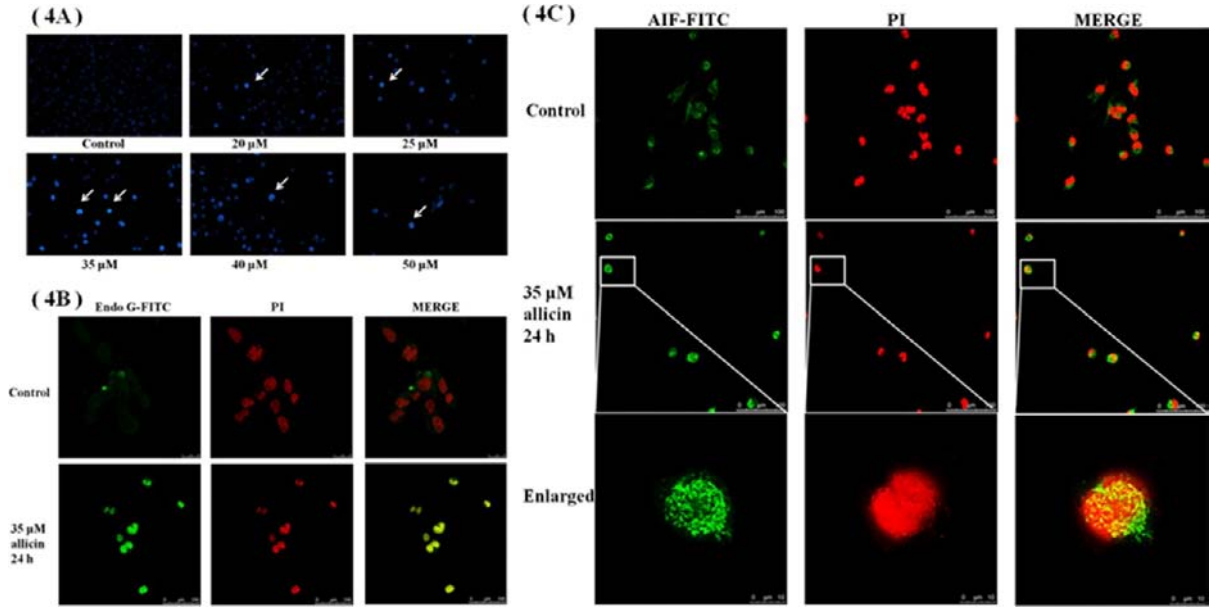

Figure 4. (A) Induction of chromatin condensation in allicin (35 μM) treated Hep 3B cells at 24 h by fluorescence microscope. Intensity of the nuclei labeled by DAPI staining is increased after 24 h of allicin treatment by excitation at 330−385 nm and emission at 420 nm (200×). (B) Endo G protein translocation into nuclei of Hep 3B cells after allicin (35 μM) treatment, as observed under a confocal laser microscope. (C) AIF protein translocation into nuclei of Hep 3B cells after allicin (35 μM) treatment, as observed under a confocal laser microscope. Scale bars are as presented.

in cell membrane, DNA, and other organelles, especially in mitochondria and ER. To examine the effect of ROS imbalance on mitochondria and to determine their involvement in the apoptosis signaling pathway, we measured mitochondrial membrane potential using flow cytometry (panels B and C of Figure 2) and inspected the protein expression of mitochondrial damage using western blotting. It is evident that MMP decreased significantly (Figure 2C) by allicin treatment, after which the mitochondria would release some apoptosis-related proteins, such as Bax, AIF, and Endo G.

Allicin treatment also increased the protein expression of pro-apoptotic protein Bax and decreased protein expression of anti-apoptotic protein Bcl-2 (Figure 3A). In addition, allicin activated the caspase-independent apoptotic pathway, as evidenced by the increase in the protein expression of AIF, Endo G, and $HtrA_2$/Omi (Figure 3A). Confocal microscopic analysis indicated the nuclei translocation of AIF and Endo G proteins (panels B and C of Figure 4). These results showed that allicin treatment induced genome digestion by AIF and Endo G protein translocation to nuclei.

Validation of Apoptosis and Autophagy in Hep 3B Cells. The protein expression levels of caspase 3, 8, and 9 increased after allicin treatment (Figure 3B), suggesting that allicin treatment triggered caspase-dependent apoptosis in Hep 3B cells. Moreover, the mRNA levels of caspase 3 and AIF also significantly increased by allicin treatment (Figure 2D). It is

dx.doi.org/10.1021/jf403241s | J. Agric. Food Chem. 2013, 61, 9839−9848

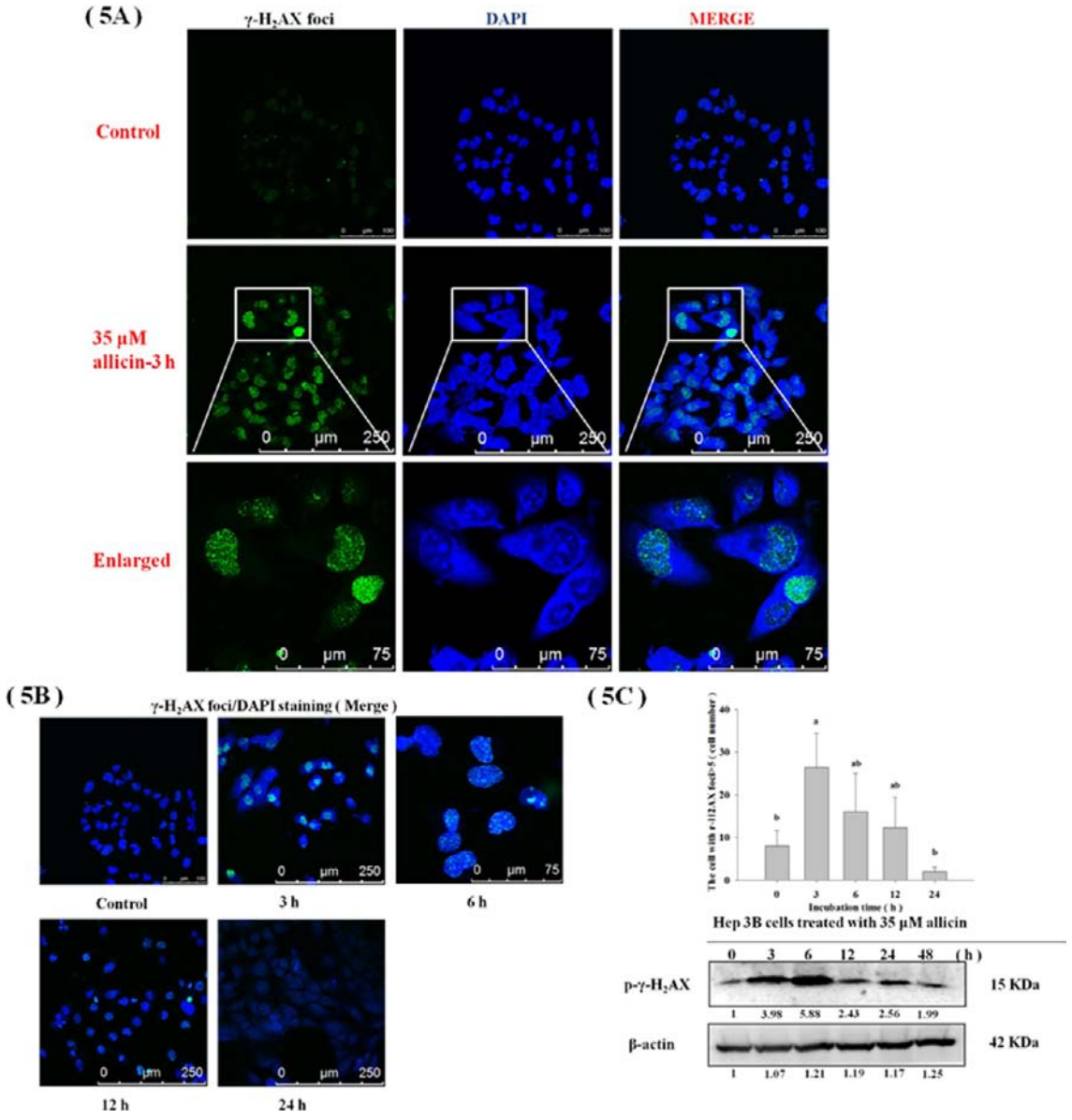

Figure 5. (A and B) Allicin induced DNA DSBs. Immunostaining of Hep 3B cells at different time points promoted the levels of γ-H_2AX foci in cell nuclei (cell nuclei was located by DAPI staining), demonstrating the role of allicin. (C) γ-H_2AX protein expression in Hep 3B cells after allicin treatment at different time intervals. Allicin (35 μM) induced Hep 3B cell protein expression of γ-H_2AX in Hep 3B significantly at 3 and 6 h but not at 12, 24, and 48 h.

quite evident from the above results that allicin induced caspase 3 and AIF in Hep 3B cells at both mRNA and protein levels. On the other hand, allicin treatment did not increase the fluorescence intensity of AO and LC-3-II-FITC punctate formation of Hep 3B cells, as shown in Figures S5 and S6 of the Supporting Information, respectively. Treatment with autophagy inhibitor 3-MA prior to allicin treatment did not repair the cell death in Hep 3B cells (see Figure S4 of the Supporting Information). Taken together, these data demonstrated that allicin did not induce autophagy but caused apoptosis in Hep 3B cells.

Apoptosis is often associated with conditions such as cell shrinkage, chromatin condensation, plasma membrane blebbing, foaming apoptosome, DNA fragmentation, and cell cycle arrest.[25] In a healthy body, apoptosis is very important in the regulation of the cell life cycle and it could maintain the normal number of healthy cells in any tissue and organ.[26] Unfortunately, cancer cells could evade apoptosis and proliferate continuously. Therefore, it is important to know how to induce apoptosis in cancer treatment.[27] However, some research work demonstrated that autophagy, also called type II programmed cell death, can be an alternative treatment in apoptosis-resistant cancer therapy.[28,29] The effect of allicin on the regulation of different modes of cell death in human liver cancer is truly worth studying.

Allicin Increased Intracellular ROS and Decreased Mitochondria Membrane Potential ($\Delta\Psi$m). To investigate the mechanism of action of allicin-induced cell death in Hep 3B cells, we examined the mitochondria membrane potential (Figure 2C and Figure S3A of the Supporting Information) and intracellular ROS by flow cytometry (Figure 2B and Figure S3B of the Supporting Information). The results showed that allicin treatment decreased $\Delta\Psi$m and increased the production of ROS levels at 1, 3, and 6 h. It is of great interest to note these

dx.doi.org/10.1021/jf403241s | J. Agric. Food Chem. 2013, 61, 9839−9848

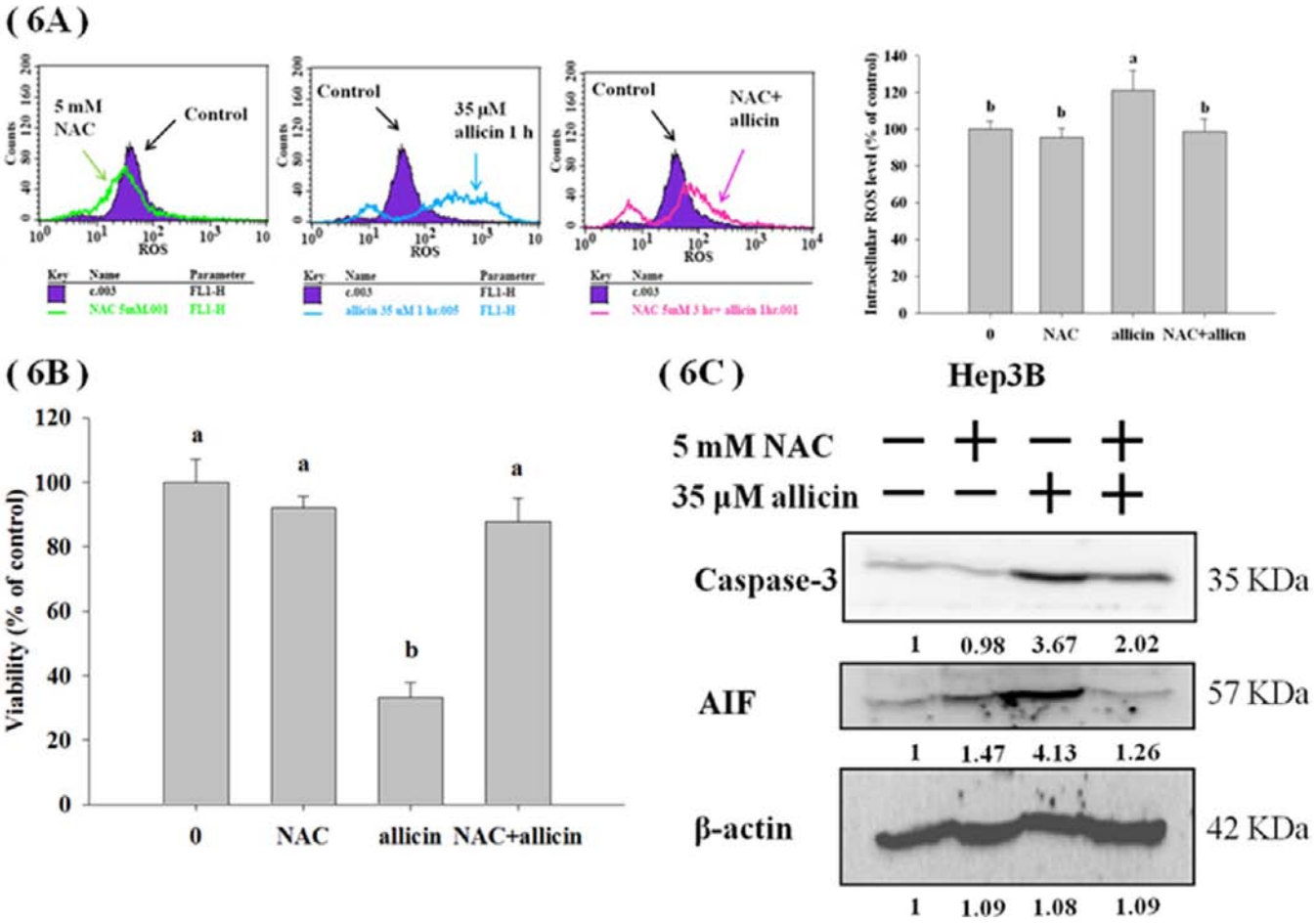

Figure 6. (A and B) Pretreatment of cells with ROS inhibitor NAC for 3 h decreases the induction of ROS by allicin and recovery of the percentage of viable cells compared to 35 μM allicin treatment alone in Hep 3B cells. Moreover, in comparison to the control group, cells treated with NAC alone indicated no changes in the caspase 3 and AIF protein levels. (C) However, NAC pretreatment accompanied with the allicin treatment group inhibited the allicin-induced protein expression of caspase 3 and AIF in Hep 3B cells. These data proved that allicin induced ROS-mediated apoptotic cell death in Hep 3B cells.

drastic changes even after short treatment intervals. Allicin treatment in Hep 3B cells may increase intracellular ROS, which damages the mitochondria and decreases the mitochondria membrane potential. Finally, ROS imbalance of cells may trigger multiple cell death pathways.[30]

To investigate the ROS imbalance control of the cell health, we studied the effect of NAC treatment. Allicin significantly induced ROS overproduction, whereas NAC pretreatment decreased the ROS induction by allicin exposure in Hep 3B cells (Figure 6A). NAC pretreatment alone did not significantly influence the viability of cells (Figure 6B) as well as the protein levels of caspase 3 and AIF (Figure 6C). Surprisingly, pretreating with NAC not only decreased the ROS overproduction induced by allicin but also recovered the cytotoxicity from allicin treatment and inhibited the induction of the protein expression of caspase 3 and AIF of allicin treatment in Hep 3B cells. Taken together, it could be inferred that NAC pretreatment could block the ROS production and keep Hep 3B cells alive, implying that ROS played a dominant role of cell survival in human liver cancer cells.

Allicin Induced DNA Breakage in Hep 3B Cells. Overproduced ROS may attack cell membrane, nucleic acid, and cause DNA damage. If DNA damage has not been repaired, it could induce cell death and apoptosis, and drugs that induce ROS production have potential for cancer therapy.[31] A DNA double-strand break (DSB) marker, γ-H_2AX, was quantified to check if it was impacted by allicin treatment. Immunostaining of allicin-treated Hep 3B cells demonstrated an increased intensity of γ-H_2AX foci in cell nuclei (Figure 5A). A significant increase in the expression of γ-H_2AX was observed at the initial stages (3 and 6 h) but not at the later stages of 12, 24, and 48 h (panels B and C of Figure 5).

In addition, we also used DAPI staining to label the nucleic acid to investigate whether allicin induced chromatin condensation. Figure 4A showed that various dosages of allicin caused chromatin condensation at 24 h in Hep 3B cells. DNA damage response (DDR) signaling is an important regulator of program cell death.[32] To examine if allicin treatment induced DRR, DNA damage generation was measured by DAPI staining and γ-H_2AX foci formation, a specific regulator of DDR signaling. It was quite evident that allicin induced DRR in Hep 3B cells (Figure 5). Also, allicin treatment significantly increased cellular production of ROS (Figure 2B). Our results indicated that allicin treatment increased the ROS production and triggered DNA damage and apoptosis in human liver cancer Hep 3B cells. To demonstrate that ROS production is an important target in allicin-treated Hep 3B cells, NAC (ROS chelating agent) treatment inhibited the induction of ROS production, caspase 3, AIF, and cell death (Figure 6). From these results, we consider that allicin truly induces Hep 3B cell

dx.doi.org/10.1021/jf403241s | J. Agric. Food Chem. 2013, 61, 9839−9848

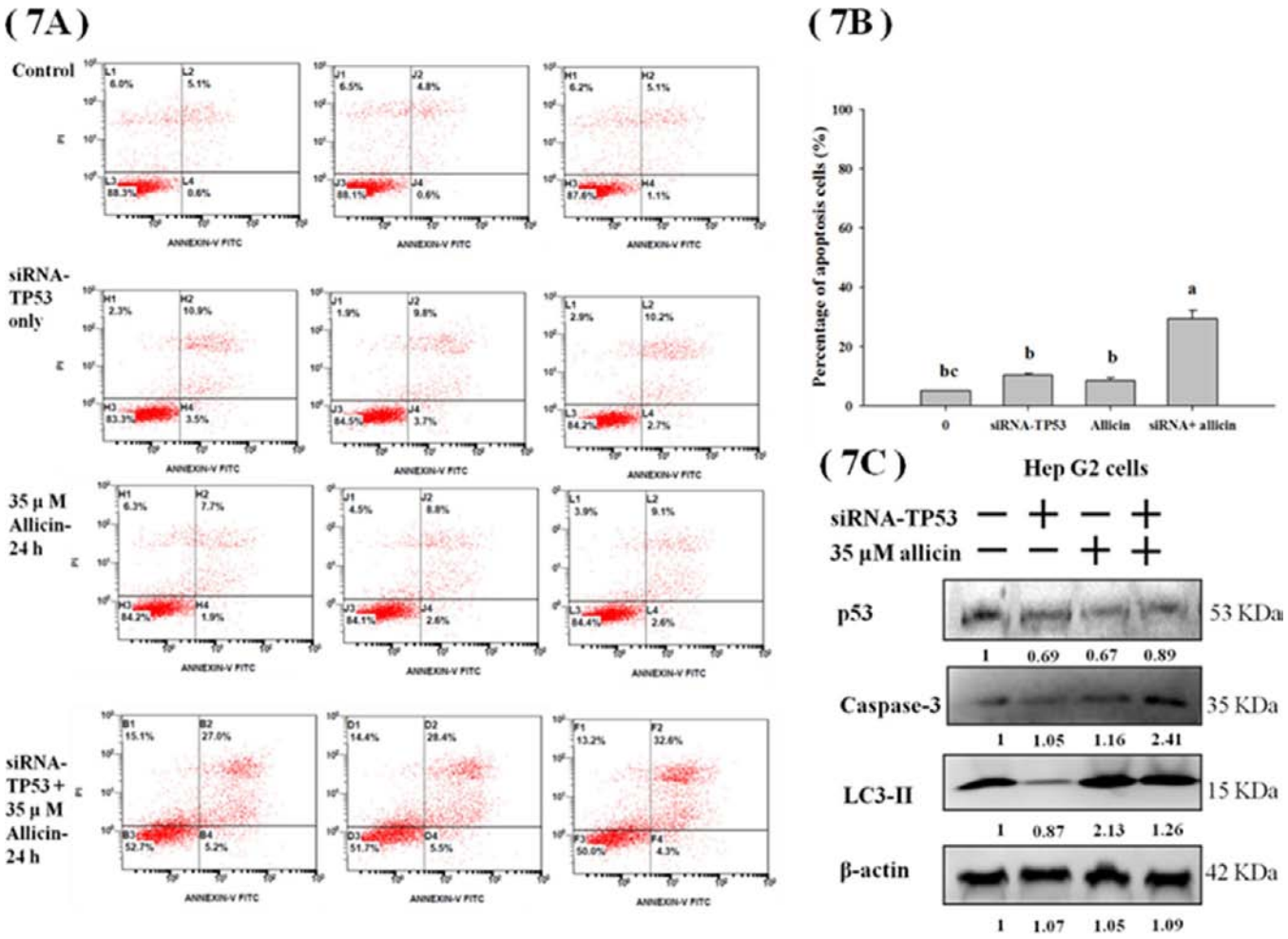

Figure 7. Percentage of apoptosis cells increase/decrease after allcin treatment in p53 siRNA silenced Hep G2 cells. (A) Flow cytometric analysis of four treatments, such as non-treatment, siRNA-TP53, allicin, and siRNA-TP53 + allicin groups. (B) Quantization of apoptotic cells analyzed by flow cytometry after allicin treatment in Hep G2 cells. (C) Protein expression of p53, caspase 3, and LC3-II in different treating groups. All results are reported as the mean ± SD, and the difference between the allicin-treated and control groups was analyzed by one-way ANOVA and Duncan's multiple comparison tests (SAS Institute, Inc., Cary, NC) to determine significant differences among treatments ($p < 0.05$).

death through provoking ROS induction. Then, the high concentration of ROS attacks the DNA to form γ-H_2AX foci.

p53 Autophagy and Apoptosis. p53 is not only a tumor suppressor protein but also is involved in various phenomena, such as mutation, carcinogenesis, endogenous or exogenous injury, and multiple cell signaling transduction, which control the life and death of a cell.[33] Some studies demonstrate that the protein level expression of p53 regulates the death process of apoptosis,[33] autophagy,[34] and necrosis.[35] Allicin induced caspase-dependent and -independent apoptosis significantly in Hep 3B ($p53^{mutation}$) cells (Figure 3).

We were curious about why allicin triggered autophagy in p53 wild type (Hep G2) cells[12] but apoptosis in p53 mutation (Hep 3B) cells and the role of the p53 gene in the regulation of cell death induced by allicin in human liver cancer cells. To thoroughly understand the role of p53, we compared Hep G2 cells with Hep 3B cells by various methods and all of our data showed that allicin induced apoptosis in Hep 3B ($p53^{mutation}$) cells, but in our previous study, we had reported that allicin induced autophagy in Hep G2 ($p53^{wild\ type}$) cells.[12] The most important difference between Hep G2 and Hep 3B cells is the presence the p53 gene in Hep G2 cells. To clarify this hypothesis, we chose to knockdown the p53 gene of Hep G2 cells. The siRNA-TP53-transfected group and allicin-treated group did not promote the percentage of annexin-V-FITC positive cells (Figure 7A). On the contrary, cells were transfected with siRNA-TP53, and the change of fresh medium with allicin treatment for 24 h exhibited a significant increase in the percentage of annexin-V-FITC cells. The data suggested that allicin induced apoptosis in p53-deficient human liver carcinoma cells but caused autophagy in p53-normal function human liver carcinoma cells.

From our results, we corroborate that, irrespective of the presence or absence of p53, allicin could regulate treatment of human liver cancer cells. Either 35 μM allicin treatment or p53 silencing in Hep G2 cells did not induce apoptosis at all, but the p53-gene-silenced Hep G2 cells when treated with 35 μM allicin significantly promoted the apoptosis cells (Figure 7B). The result explains how allicin regulates different modes of cell death by p53 expression in human liver cancer. We validated the p53 protein levels in the knocked down cell lines (Figure 7C) and observed inhibition of LC3-II protein expression but increased caspase 3 production on allicin treatment.

In summary, allicin treatment increases production of ROS and triggers DNA damage and caspase-dependent and -independent apoptosis in Hep 3B ($p53^{mutation}$) human liver

dx.doi.org/10.1021/jf403241s | J. Agric. Food Chem. 2013, 61, 9839−9848

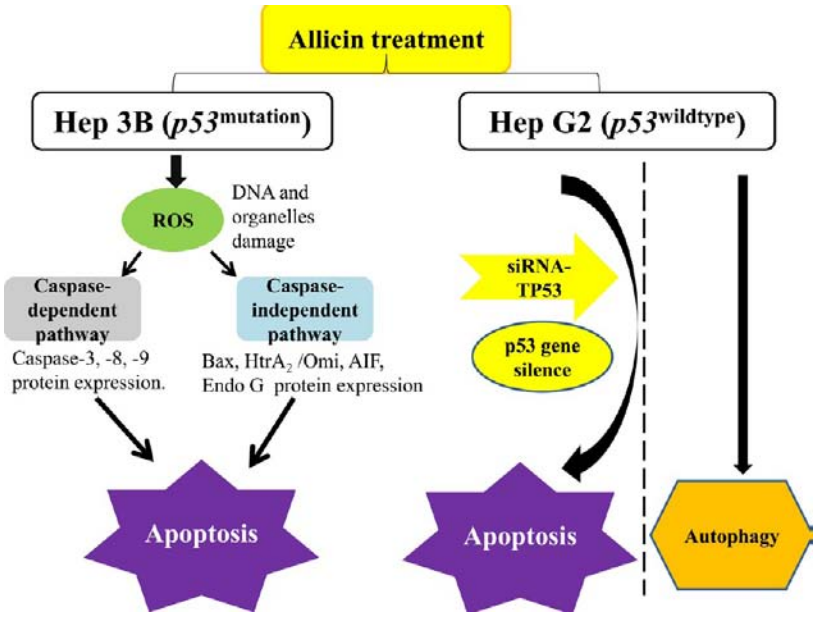

Figure 8. In summary, allicin treatment increases production of ROS and triggers DNA damage and caspase-dependent and -independent apoptosis in Hep 3B ($p53^{mutation}$) human liver cancer cells. Moreover, our results prove that p53-silenced Hep G2 cells have the same response as Hep 3B cells after allicin exposure and trigger apoptosis.

cancer cells (Figure 8). Although our previous study showed that allicin induced autophagy in Hep G2 ($p53^{wild\ type}$) cells, p53 knocked down Hep G2 cells had the same response as Hep 3B cells after allicin exposure (Figure 8). We consider that allicin could regulate the apoptotic or autophagic cell death pathway through the p53 gene in both transcription and translation levels. Moreover, the existence of p53 may guide cancer cells to autophagy or lead other cancer cells without p53 to apoptosis in some therapies. All of the results demonstrate that allicin is a powerful active component for potential complementary therapy no matter in p53-normal or p53-deficient liver carcinoma cells through different cell death mechanisms *in vitro*.

■ ASSOCIATED CONTENT

Supporting Information

Effect of allicin on the distribution of the cell cycle in Hep 3B cells after 24 h (Figure S1), annexin V/PI staining analysis of Hep 3B cells with allicin at different time intervals (Figure S2), distribution of (A) mitochondria membrane potential ($\Delta\Psi$m) and (B) ROS production of Hep 3B cells with 35 μM allicin at different time intervals (Figure S3), viability of 35 μM allicin (35 μM) treated Hep 3B cells at 24 h after 2 h of pretreatment with 3-MA (2 mM) (Figure S4), autophagic assay measured by AO staining after 35 μM allicin treatment in Hep 3B cells at various times (Figure S5), and autophagosome formation analyzed by LC3-II-FITC punctate after allicin treatment in Hep 3B cells in various times (Figure S6). This material is available free of charge via the Internet at http://pubs.acs.org.

■ AUTHOR INFORMATION

Corresponding Author

*Telephone: 886-2-33664129. Fax: 886-2-2362-0849. E-mail: lysheen@ntu.edu.tw.

Funding

This study was supported in part by a grant from the National Science Council of Taiwan (NSC-99-2321-B-002-042) and the National Taiwan University (Aim for Top University Program 102R-7620), Taiwan.

Notes

The authors declare no competing financial interest.

■ ABBREVIATIONS USED

ROS, reactive oxygen species; $\Delta\Psi$m, MMP, mitochondrial membrane potential; PCD, program cell death; AIF, apoptotic-inducing factor; Endo G, endonuclease G; DMSO, dimethyl sulfoxide; PI, propidium iodide; NAC, *N*-acetylcysteine; 3-MA, 3-methyladenine; LC3, MAP-1, microtubule-associated protein 1 light chain 3; Bax, Bcl-2-associated X protein; Bcl-2, B-cell lymphoma 2; PBS, phosphate-buffered saline; AO, acridine orange; qRT-PCR, quantitative real-time polymerase chain reaction; DSB, DNA double-strand break; ER, endoplasmic reticulum; FACS, fluorescence-activated cell sorting

■ REFERENCES

(1) Rich, G. E. Garlic an antibiotic? *Med. J. Aust.* **1982**, *1* (2), 60.

(2) Lee, M. H.; Kim, Y. M.; Kim, S. G. Efficacy and tolerability of diphenyl-dimethyl-dicarboxylate plus garlic oil in patients with chronic hepatitis. *Int. J. Clin. Pharmacol. Ther.* **2012**, *50* (11), 778−786.

(3) Kiesewetter, H.; Jung, F.; Jung, E. M.; Mroweitz, C.; Koscielny, J.; Wenzel, E. Effect of garlic on platelet aggregation in patients with increased risk of juvenile ischaemic attack. *Eur. J. Clin. Pharmacol.* **1993**, *45* (4), 333−336.

(4) Gorinstein, S.; Jastrzebski, Z.; Namiesnik, J.; Leontowicz, H.; Leontowicz, M.; Trakhtenberg, S. The atherosclerotic heart disease and protecting properties of garlic: Contemporary data. *Mol. Nutr. Food Res.* **2007**, *51* (11), 1365−1381.

(5) Matsuura, N.; Miyamae, Y.; Yamane, K.; Nagao, Y.; Hamada, Y.; Kawaguchi, N.; Katsuki, T.; Hirata, K.; Sumi, S.; Ishikawa, H. Aged garlic extract inhibits angiogenesis and proliferation of colorectal carcinoma cells. *J. Nutr.* **2006**, *136* (Supplement 3), 842S−846S.

(6) Raghu, R.; Liu, C. T.; Tsai, M. H.; Tang, X.; Kalari, K. R.; Subramanian, S.; Sheen, L. Y. Transcriptome analysis of garlic-induced hepatoprotection against alcoholic fatty liver. *J. Agric. Food Chem.* **2012**, *60* (44), 11104−11119.

(7) Oommen, S.; Anto, R. J.; Srinivas, G.; Karunagaran, D. Allicin (from garlic) induces caspase-mediated apoptosis in cancer cells. *Eur. J. Pharmacol.* **2004**, *485* (1−3), 97−103.
(8) Chen, R. J.; Tsai, S. J.; Ho, C. T.; Pan, M. H.; Ho, Y. S.; Wu, C. H.; Wang, Y. J. Chemopreventive effects of pterostilbene on urethane-induced lung carcinogenesis in mice via the inhibition of EGFR-mediated pathways and the induction of apoptosis and autophagy. *J. Agric. Food Chem.* **2012**, *60* (46), 11533−11541.
(9) Wang, J.; Yi, J. Cancer cell killing via ROS: To increase or decrease, that is the question. *Cancer Biol. Ther.* **2008**, *7* (12), 1875−1884.
(10) Yang, T. P.; Lee, H. J.; Ou, T. T.; Chang, Y. J.; Wang, C. J. Mulberry leaf polyphenol extract induced apoptosis involving regulation of adenosine monophosphate-activated protein kinase/fatty acid synthase in a p53-negative hepatocellular carcinoma cell. *J. Agric. Food Chem.* **2012**, *60* (27), 6891−6897.
(11) Druesne, N.; Pagniez, A.; Mayeur, C.; Thomas, M.; Cherbuy, C.; Duee, P. H.; Martel, P.; Chaumontet, C. Diallyl disulfide (DADS) increases histone acetylation and p21(waf1/cip1) expression in human colon tumor cell lines. *Carcinogenesis* **2004**, *25* (7), 1227−1236.
(12) Chu, Y. L.; Ho, C. T.; Chung, J. G.; Rajasekaran, R.; Sheen, L. Y. Allicin induces p53-mediated autophagy in Hep G2 human liver cancer cells. *J. Agric. Food Chem.* **2012**, *60* (34), 8363−8371.
(13) Huang, S. H.; Wu, L. W.; Huang, A. C.; Yu, C. C.; Lien, J. C.; Huang, Y. P.; Yang, J. S.; Yang, J. H.; Hsiao, Y. P.; Wood, W. G.; Yu, C. S.; Chung, J. G. Benzyl isothiocyanate (BITC) induces G2/M phase arrest and apoptosis in human melanoma A375.S2 cells through reactive oxygen species (ROS) and both mitochondria-dependent and death receptor-mediated multiple signaling pathways. *J. Agric. Food Chem.* **2012**, *60* (2), 665−675.
(14) Kuo, J. H.; Chu, Y. L.; Yang, J. S.; Lin, J. P.; Lai, K. C.; Kuo, H. M.; Hsia, T. C.; Chung, J. G. Cantharidin induces apoptosis in human bladder cancer TSGH 8301 cells through mitochondria-dependent signal pathways. *Int. J. Oncol.* **2010**, *37* (5), 1243−1250.
(15) Livak, K. J.; Schmittgen, T. D. Analysis of relative gene expression data using real-time quantitative PCR and the $2^{-\Delta\Delta C_T}$ method. *Methods* **2001**, *25* (4), 402−408.
(16) Cui, W.; Taub, D. D.; Gardner, K. qPrimerDepot: A primer database for quantitative real time PCR. *Nucleic Acids Res.* **2007**, *35* (Database Issue), D805−D809.
(17) Wang, X.; Jiao, F.; Wang, Q. W.; Wang, J.; Yang, K.; Hu, R. R.; Liu, H. C.; Wang, H. Y.; Wang, Y. S. Aged black garlic extract induces inhibition of gastric cancer cell growth in vitro and in vivo. *Mol. Med. Rep.* **2012**, *5* (1), 66−72.
(18) Bat-Chen, W.; Golan, T.; Peri, I.; Ludmer, Z.; Schwartz, B. Allicin purified from fresh garlic cloves induces apoptosis in colon cancer cells via Nrf2. *Nutr. Cancer* **2010**, *62* (7), 947−957.
(19) Wang, H. C.; Pao, J.; Lin, S. Y.; Sheen, L. Y. Molecular mechanisms of garlic-derived allyl sulfides in the inhibition of skin cancer progression. *Ann. N. Y. Acad. Sci.* **2012**, *1271*, 44−52.
(20) Modem, S.; Dicarlo, S. E.; Reddy, T. R. Fresh garlic extract induces growth arrest and morphological differentiation of MCF7 breast cancer cells. *Genes Cancer* **2012**, *3* (2), 177−186.
(21) Ouyang, L.; Shi, Z.; Zhao, S.; Wang, F. T.; Zhou, T. T.; Liu, B.; Bao, J. K. Programmed cell death pathways in cancer: A review of apoptosis, autophagy and programmed necrosis. *Cell Proliferation* **2012**, *45* (6), 487−498.
(22) Wu, P. P.; Chung, H. W.; Liu, K. C.; Wu, R. S.; Yang, J. S.; Tang, N. Y.; Lo, C.; Hsia, T. C.; Yu, C. C.; Chueh, F. S.; Lin, S. S.; Chung, J. G. Diallyl sulfide induces cell cycle arrest and apoptosis in HeLa human cervical cancer cells through the p53, caspase- and mitochondria-dependent pathways. *Int. J. Oncol.* **2011**, *38* (6), 1605−1613.
(23) Chiu, T. H.; Lan, K. Y.; Yang, M. D.; Lin, J. J.; Hsia, T. C.; Wu, C. T.; Yang, J. S.; Chueh, F. S.; Chung, J. G. Diallyl sulfide promotes cell-cycle arrest through the p53 expression and triggers induction of apoptosis via caspase- and mitochondria-dependent signaling pathways in human cervical cancer Ca Ski cells. *Nutr. Cancer* **2013**, *65* (3), 505−514.
(24) Gebhardt, R.; Beck, H.; Wagner, K. G. Inhibition of cholesterol biosynthesis by allicin and ajoene in rat hepatocytes and HepG2 cells. *Biochim. Biophys. Acta* **1994**, *1213* (1), 57−62.
(25) Mirandola, P.; Gobbi, G.; Sponzilli, I.; Malinverno, C.; Cavazzoni, A.; Alfieri, R.; Petronini, P. G.; Vitale, M. TRAIL-induced apoptosis of FHIT-negative lung cancer cells is inhibited by FHIT re-expression. *J. Cell. Physiol.* **2009**, *220* (2), 492−498.
(26) Harada, K.; Iwata, M.; Kono, N.; Koda, W.; Shimonishi, T.; Nakanuma, Y. Distribution of apoptotic cells and expression of apoptosis-related proteins along the intrahepatic biliary tree in normal and non-biliary diseased liver. *Histopathology* **2000**, *37* (4), 347−354.
(27) Liu, Z.; Li, D.; Zheng, X.; Wang, E.; Wang, J. Selective induction of apoptosis: Promising therapy in pancreatic cancer. *Curr. Pharm. Des.* **2013**, *19* (12), 2259−2268.
(28) Carew, J. S.; Kelly, K. R.; Nawrocki, S. T. Autophagy as a target for cancer therapy: New developments. *Cancer Manage. Res.* **2012**, *4*, 357−365.
(29) Igney, F. H.; Krammer, P. H. Death and anti-death: Tumour resistance to apoptosis. *Nat. Rev. Cancer* **2002**, *2* (4), 277−288.
(30) Chen, Y.; McMillan-Ward, E.; Kong, J.; Israels, S. J.; Gibson, S. B. Oxidative stress induces autophagic cell death independent of apoptosis in transformed and cancer cells. *Cell Death Differ.* **2008**, *15* (1), 171−182.
(31) Ralph, S. J.; Rodriguez-Enriquez, S.; Neuzil, J.; Saavedra, E.; Moreno-Sanchez, R. The causes of cancer revisited: "Mitochondrial malignancy" and ROS-induced oncogenic transformation—Why mitochondria are targets for cancer therapy. *Mol. Aspects Med.* **2010**, *31* (2), 145−170.
(32) Kuo, L. J.; Yang, L. X. Gamma-H2AX—A novel biomarker for DNA double-strand breaks. *In Vivo* **2008**, *22* (3), 305−309.
(33) Vousden, K. H.; Lu, X. Live or let die: The cell's response to p53. *Nat. Rev. Cancer* **2002**, *2* (8), 594−604.
(34) Sui, X.; Jin, L.; Huang, X.; Geng, S.; He, C.; Hu, X. p53 signaling and autophagy in cancer: A revolutionary strategy could be developed for cancer treatment. *Autophagy* **2011**, *7* (6), 565−571.
(35) Vaseva, A. V.; Marchenko, N. D.; Ji, K.; Tsirka, S. E.; Holzmann, S.; Moll, U. M. p53 opens the mitochondrial permeability transition pore to trigger necrosis. *Cell* **2012**, *149* (7), 1536−1548.